

REPORT DOCUMENTATION PAGE

Form Approved
OMB No. 0704-0188

Public reporting burden for this collection of information is estimated to average 1 hour per response, including the time for reviewing instructions, searching existing data sources, gathering and maintaining the data needed, and completing and reviewing this collection of information. Send comments regarding this burden estimate or any other aspect of this collection of information, including suggestions for reducing this burden to Department of Defense, Washington Headquarters Services, Directorate for Information Operations and Reports (0704-0188), 1215 Jefferson Davis Highway, Suite 1204, Arlington, VA 22202-4302. Respondents should be aware that notwithstanding any other provision of law, no person shall be subject to any penalty for failing to comply with a collection of information if it does not display a currently valid OMB control number. **PLEASE DO NOT RETURN YOUR FORM TO THE ABOVE ADDRESS.**

| | | | | | |
|--|--------------------|--|-----------------------------------|---|--|
| 1. REPORT DATE (DD-MM-YYYY) 07-07-2005 | | 2. REPORT TYPE Journal Article | | 3. DATES COVERED (From - To) | |
| 4. TITLE AND SUBTITLE Solid State Thermochemical Decomposition of Neat 1,3,5,5-Tetranitrohexahydropyrimidine (DNNC) and its DNNC-d₆ Perdeuterio-Labeled Analogue (PREPRINT) | | | | 5a. CONTRACT NUMBER | |
| | | | | 5b. GRANT NUMBER | |
| | | | | 5c. PROGRAM ELEMENT NUMBER | |
| 6. AUTHOR(S) Scott A. Hendrickson (Pt. Loma Nazarene Univ.) and Scott A. Shackelford (AFRL/PRSP) | | | | 5d. PROJECT NUMBER 5026 | |
| | | | | 5e. TASK NUMBER 0541 | |
| | | | | 5f. WORK UNIT NUMBER | |
| 7. PERFORMING ORGANIZATION NAME(S) AND ADDRESS(ES) Air Force Research Laboratory (AFMC) AFRL/PRSP 10 E. Saturn Blvd. Edwards AFB CA 93524-7680 | | | | 8. PERFORMING ORGANIZATION REPORT NUMBER AFRL-PR-ED-JA-2005-273 | |
| 9. SPONSORING / MONITORING AGENCY NAME(S) AND ADDRESS(ES) Air Force Research Laboratory (AFMC) AFRL/PRS 5 Pollux Drive Edwards AFB CA 93524-7048 | | | | 10. SPONSOR/MONITOR'S ACRONYM(S) | |
| | | | | 11. SPONSOR/MONITOR'S NUMBER(S) AFRL-PR-ED-JA-2005-273 | |
| 12. DISTRIBUTION / AVAILABILITY STATEMENT Approved for public release; distribution unlimited | | | | | |
| 13. SUPPLEMENTARY NOTES Submitted to Thermochimica Acta | | | | | |
| 14. ABSTRACT The solid state thermochemical decomposition kinetics and activation energy of neat 1,3,5,5-tetranitrohexahydropyrimidine (DNNC) and its DNNC-d ₆ deuterium labeled analogue were obtained by isothermal differential scanning calorimetry (IDSC) at 142, 145, and 148 °C. Global rate constants and kinetic deuterium isotope effect (KDIE) data from the exothermic decomposition process suggest that homolytic C-H bond rupture, in one or both types of chemically non-equivalent methylene (-CH ₂) groups of the DNNC ring structure, constitutes the exothermic rate-controlling step. A DNNC-d ₆ energy of activation equal to 115 kJ/mole was determined for this initial autocatalytic exothermic energy release from which a 106 kJ/mol activation energy was calculated for unlabeled DNNC. This exothermic autocatalytic decomposition process follows an extended endothermic induction period for DNNC which shows a higher 128 kJ/mole activation energy during which a catalytic initiating species may form by a rate-controlling step different from C-H bond rupture. | | | | | |
| 15. SUBJECT TERMS | | | | | |
| 16. SECURITY CLASSIFICATION OF: | | | 17. LIMITATION OF ABSTRACT | 18. NUMBER OF PAGES | 19a. NAME OF RESPONSIBLE PERSON |
| a. REPORT | b. ABSTRACT | c. THIS PAGE | | | Scott A. Shackelford |
| Unclassified | Unclassified | Unclassified | A | 35 | 19b. TELEPHONE NUMBER <i>(include area code)</i> (661) 275-5847 |

Solid State Thermochemical Decomposition of Neat
1,3,5,5-Tetranitrohexahydropyrimidine (DNNC) and
Its DNNC-d₆ Perdeuterio-Labeled Analogue

Scott A. Hendrickson^{+,1a} and Scott A. Shackelford^{#, 1b,c*}

⁺ *Department of Chemistry, Pt. Loma Nazarene University, San Diego, CA 92106-2899 (USA)*

[#] *Air Force Research Laboratory, AFRL/PRSP, Edwards AFB, CA 93524-7680 (USA)*

Abstract

The solid state thermochemical decomposition kinetics and activation energy of neat 1,3,5,5-tetranitrohexahydropyrimidine (DNNC) and its DNNC-d₆ deuterium labeled analogue were obtained by isothermal differential scanning calorimetry (IDSC) at 142, 145, and 148 °C. Global rate constants and kinetic deuterium isotope effect (KDIE) data from the exothermic decomposition process suggest that homolytic C-H bond rupture, in one or both types of chemically non-equivalent methylene (-CH₂) groups of the DNNC ring structure, constitutes the exothermic rate-controlling step. A DNNC-d₆ energy of activation equal to 115 kJ/mole was determined for this initial autocatalytic exothermic energy release from which a 106 kJ/mol activation energy was calculated for unlabeled DNNC. This exothermic autocatalytic decomposition process follows an extended endothermic induction period for DNNC which shows a higher 128 kJ/mole activation energy during which a catalytic initiating species may form by a rate-controlling step different from C-H bond rupture.

Keywords: 1,3,5,5-Tetranitrohexahydropyrimidine, DNNC, Solid State Decomposition, Deuterium Isotope Effect, KDIE

*Corresponding author; e-mail: scott.shackelford@edwards.af.mil

Distribution A: Approved for public release; distribution unlimited.

1. Introduction

Global, heterogeneous reaction kinetics obtained via isothermal differential scanning calorimeter (IDSC) analyses often are ignored in favor of highly-defined homogeneous kinetic studies that measure specific reaction steps. However, the global kinetics obtained from liquid and solid state thermochemical decomposition processes with neat high energy compounds provide important data for practical technology and safety considerations.[2] An isothermal DSC analysis aptly demonstrated this point when the resultant global kinetics data from the solid state decomposition of 1,3,5-triamino-2,4,6-trinitrobenzene (TATB) was used to predict the critical temperature needed to initiate a thermal explosion event.[3] The critical temperature of an energetic compound defines the lowest constant surface temperature at which a compound, given a specific size, shape, and composition, can self-heat to a catastrophic event. When the global kinetic rate constant for this solid state TATB decomposition process was substituted into the Frank-Kamenetskii equation, the predicted 354 °C critical temperature matched its experimentally-determined value.[3]

Factors influencing global solid heterogeneous kinetic rates are decidedly different from those encountered in less complex homogeneous kinetic studies. Global reaction kinetics in condensed phase thermochemical decomposition heavily involve complex bimolecular reaction processes,[4] and in the solid state, describe reactions occurring within a thin zone of reactant-product contact that advance into the non-decomposed interior of the particle.[2] Other factors uniquely influencing global heterogeneous solid compound kinetic measurements include melting, impurities, and crystal defects.[2] For these reasons, when conducting kinetic deuterium isotope effect-based (KDIE) thermochemical decomposition

analyses like those described in this investigation, it is important, whenever possible, to synthesize and prepare non-labeled and analogous deuterium-labeled compounds in an identical manner. This action ensures any kinetic rate differences found result solely from the deuterium atom substitution.[5]

Given the importance of global heterogeneous kinetic and mechanistic data with energetic compounds, the solid state thermochemical decomposition process of 1,3,5,5-tetranitro-hexahydropyrimidine (DNNC) and its DNNC-d₆ deuterium labeled analogue were investigated by isothermal DSC analysis using the kinetic deuterium isotope effect (KDIE) approach. A maximum sensitivity setting was used for the DSC instrument in order to detect minute curve deflections over short time intervals. The global reaction rate constants, resultant energies of activation, and the rate-controlling bond ruptures regulating the energy release rate for the neat solid state DNNC thermochemical decomposition process were determined.

DNNC is comprised of a unique heterocyclic hybrid chemical structure that incorporates features found in both high energy geminal dinitroalkane and cyclic nitramine compounds (Fig. 1). The DNNC molecule contains two types of methylene groups [-CH₂-] sandwiched between two different energetic structural sites. One non-equivalent -CH₂- group is sandwiched between two nitrated N atoms [N-NO₂] at the ring 1 and 3-positions, and two chemically equivalent -CH₂- groups each flank the geminal dinitro-substituted ring carbon atom [C(NO₂)₂] at the 5-position. First synthesized in 1982,[6,7] the DNNC[8] hybrid structure is a high energy pseudo-nitramine with an impact sensitivity significantly lower than that exhibited by the structurally related cyclic RDX nitramine. The explosive initiation sensitivity of DNNC resembles that of the more stable nitroaromatic TNT molecule, but when

initiated, its detonation energy is significantly higher than TNT and rivals the RDX nitramine.[6] Thus,

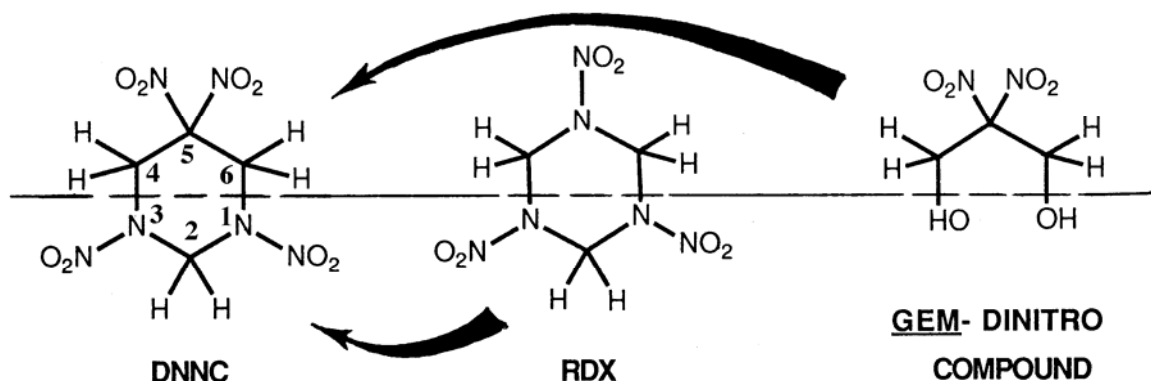


Fig. 1. Intramolecular hybrid structure of the DNNC molecule.

the DNNC pseudo nitramine exhibits energy and sensitivity properties associated with both nitramine and nitroaromatic compounds.

DNNC thermochemical stability also is similar to TNT in that it melts without noticeable or significant decomposition. A standard scanning DSC study used to determine the heat of fusion at its 154.8 to 156.2 °C melting point revealed no significant DNNC sample decomposition. Permitting the melted DNNC sample to re-solidify, then conducting an IDSC liquid thermochemical decomposition run at 176 °C gave virtually the same thermogram and heat of decomposition energy output as did a fresh DNNC sample at the same temperature.[9] Conversely, the symmetrical, cyclic six-membered RDX nitramine and its eight-membered HMX homologue undergo thermochemical decomposition during melting or liquefaction so rapidly that their heat of fusion cannot be determined.[9]

Two thermal decomposition studies have been reported for DNNC. One decomposition was conducted in solvent (THF) at 105 °C at high pressure (1.1 GPa) conditions. Under

diluted solvent conditions, an apparent unimolecular process was inferred that produced a facile elimination of HNO_2 with no rate-controlling step reported.[10] Thermochemical decomposition processes conducted in solvents are quite different from the ambient pressure, neat solid state DNNC thermochemical decomposition conditions of this investigation where bimolecular processes likely predominate.

A second thermochemical decomposition investigation with neat DNNC and several of its 5-substituted (Fig. 1) derivatives employed T-Jump/FTIR and Raman spectroscopy analyses at 0.5MPa and 350 °C. Results suggested that the substituted groups at the 5-position largely control the pathway followed by the predominantly bimolecular decomposition process and determine the gaseous products observed.[11] Once again, no rate-controlling step was identified. While structural features at the 5-position may determine a specific pathway for the thermochemical decomposition process, homolytic bond rupture kinetically controls the rate at which this DNNC decomposition pathway proceeds. The rate-controlling bond rupture, and the activation energy required to initiate it, recently were presented for the both the DNNC solid and liquid state decomposition processes in an abbreviated format.[12]

Identification of this rate-controlling chemical bond rupture during the ambient pressure thermochemical decomposition process is a key mechanistic feature of energetic compound behavior. The same rate-controlling bond rupture seen in the thermochemical decomposition process for both nitroaromatic and nitramine compounds mirrors that found in the more drastic high pressure and temperature combustion and explosion events.[13] Indeed, it also appears this rate-controlling chemical bond rupture is a key mechanistic step in energetic compound global initiation and sensitivity properties.[14]

Amid the myriad of complex simultaneous and sequential chemical reactions that proceed during the thermochemical decomposition process, the kinetic deuterium isotope effect (KDIE) approach, used with ambient pressure IDSC analysis, has identified this critical rate-controlling bond rupture, first with liquid TNT (2,4,6-trinitrotoluene),[18] and subsequently, for solid TATB (1,3,5-triamino-2,4,6-trinitrobenzene),[3] liquid and solid HMX (octahydro-1,3,5,7-tetranitro-1,3,5,7-tetrazocine),[15] liquid RDX (1,3,5-trinitrohexahydro-1,3,5-triazine),[19] and their respective deuterium-labeled TNT- α -d₃, TATB-d₆, HMX-d₈, RDX-d₆ analogues. The rate-controlling step also has been determined using isothermal thermal gravimetric analyses (TGA) with HMX/HMX-d₈ and RDX/RDX-d₆ nitramines since they produce mainly gaseous products during their liquid and solid state thermochemical decomposition processes.[20] While the rate-controlling bond rupture may or may not constitute the first homolytic bond rupture during a complex thermochemical decomposition process, this bond rupture occurs during the slowest step of a coherent, steady-state reaction. This key reaction and its rate-controlling bond rupture predominate over all other reactions during a specific portion of the complex decomposition process, and thereby, kinetically regulate the overall rate at which the process proceeds.

In every case, the same rate-controlling bond rupture found in the ambient pressure thermochemical decomposition process for a given energetic compound[3,13,17-20] also appears to be the rate-controlling step for high pressure combustion(5,13,21) and the predominant rate-controlling feature in explosive initiation events[3,13,20,22-27]

Using the maximum IDSC instrument sensitivity settings, this report investigates the ambient pressure solid state thermochemical decomposition mechanism of neat DNNC

between 142 to 148 °C below its melting point range of 154.8-156.2 °C.[9] Following a three to five hour endothermic induction period, DNNC undergoes a very slow but significant exothermic thermochemical decomposition process. IDSC analyses conducted with DNNC and DNNC-d₆, coupled with the kinetic deuterium isotope effect (KDIE) approach, identifies the rate-controlling bond rupture that governs the rate at which the solid state decomposition proceeds and permits its energy of activation to be determined.

2. Experimental

2.1 Instrumental and Chemical Details

The IDSC thermochemical decomposition curves were obtained using a PerkinElmer DSC 7 instrument set to its maximum sensitivity. PerkinElmer stainless steel large volume capsules (LVC), part no. 0319-1526 (top) and 0319-1525 (bottom) were used without Viton O-ring seals, part no. 0319-1535. DNNC and DNNC-d₆ sample sizes ranging from 1.50 to 1.54 mg were weighed into the LVC capsules and then sealed in the open atmosphere. During the IDSC thermochemical decomposition, the sealed capsules were under a stream of nitrogen gas using the highest instrumental sensitivity setting immediately following a contractor-accomplished instrumental calibration and fine tuning service call. To ensure utmost accuracy, the DSC 7 temperature was calibrated with indium (mp 156.60 °C) prior to each IDSC sample run. A total of 32 IDSC runs were conducted. Six runs were conducted on DNNC at 148 °C and 145 °C, while five runs were conducted each on DNNC at 142 °C and DNNC-d₆ at 148 °C, 145 °C, and 142 °C. Both DNNC and DNNC-d₆ were synthesized, isolated, purified, and characterized in an identical manner and have been reported in detail.[15]

2.2 Thermogram Curve Evaluation

The thermochemical decomposition curves for both DNNC and DNNC-d₆ were evaluated using the $\delta\alpha/\delta t = k\alpha(1-\alpha)$ autocatalytic rate plot equation where (α) is the mole fraction of decomposed DNNC at any given time (t) [3,13,16,17]. To approximate the instantaneous $\delta\alpha/\delta t$ area of curve change, the average change in area (Δa) divided by the time interval distances (Δt) was used ($\Delta a/\Delta t$). Progressive summation of all individual segmented areas along the thermogram curve ($\sum \Delta a$) gives the total area under the curve (A), while progressive summation of these areas up to a certain point in time ($\Delta a_0 \dots \Delta a_n$) gives the amount of decomposed sample (a_n) at that specific time. The mole fraction (α) of decomposed DNNC remaining is given by the fraction of the area under the entire curve up to a certain point ($\alpha = a_n/A$). A graphics plot of $\Delta a/\Delta t$ versus $\alpha(1-\alpha)$ defines an autocatalytic rate behavior where the slope of any linear portion on the curve gives the kinetic rate constant (k).

Previously, individual $\Delta a/\Delta t$ areas have been determined using the curve height above the baseline (h) at given time (t) along the thermogram curve. Because IDSC measures the total heat evolved during the decomposition process, and because this heat evolution is proportional to the global rate at which the sample chemically reacts, the overall rate of decomposition is described by the following approximation: $\delta\alpha/\delta t = \text{height (h) divided by the corresponding time along the curve (t)}$. Thus, $\delta\alpha/\delta t = \Delta a/\Delta t = h/t$, or $\delta\alpha/\delta t = h/t$ because h approximates the very small width of the individual $\Delta a/\Delta t$ segment.[16]

This height-based approximation has successfully been used for autocatalytic rate plots of IDSC curves where the thermochemical decomposition occurs over a period of minutes.[3,12,13-19] However, these solid state DNNC and DNNC-d₆ thermochemical

decomposition processes occurred over many hours (eg. nearly 14 hours at 145 °C).[12]

Because the IDSC instrumentation software could plot only a finite number of data points, a long decomposition process possibly gave much larger Δt distance intervals and resultant Δa_n areas. Consequently, the height-based approximation approach, with its very narrow Δt widths and potentially much smaller calculated Δa_n values, was not used. Rather, areas for Δa_n were calculated with measured Δt interval distances using a modification of Simpson's Rule.

Simpson's Rule determines individual areas (Δa_n) at corresponding time distance intervals (Δt_n) located along the baseline of the thermochemical decomposition curve. The standard Simpson's Rule divides a continuous curve into equally distributed time intervals (Δt), and processes these time intervals in pairs ($\Delta t_n, \Delta t_{n+1}$). Each time interval pair is defined using three data points: (P_1) the start of the first interval, (P_2) the end of the first interval and beginning of the second interval, and (P_3) the end of the second interval. Simpson's Rule uses these three points (P_{1-3}) to approximate the polynomial area under the decomposition curve ($\Delta a_n + \Delta a_{n+1}$) for the pair of time intervals ($\Delta t_n + \Delta t_{n+1}$). Using this approach, the area of the entire curve (A), or a large portion of it, may be approximated by aggregating the approximated areas ($\sum \Delta a_n$) of each pair of time intervals along the curve.

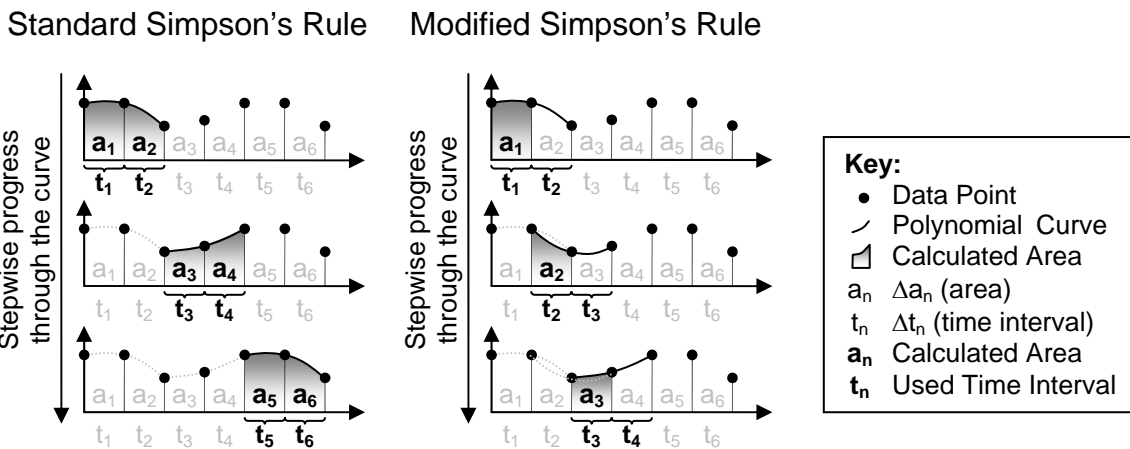


Fig. 2. Standard and modified Simpson's Rules.

The standard Simpson's Rule requires the use of pairs of time intervals, which limits the flexibility of the approach because it requires an even number of time intervals to be considered. To rectify this, Simpson's Rule was modified (see Fig. 2) so that, as before, two time intervals are used ($\Delta t_n, \Delta t_{n+1}$) to approximate the original decomposition curve, but unlike before, only the area under the curve of the first interval (Δa_n) is approximated from this curve. To calculate the area for the next interval (Δa_{n+1}), the modified Simpson's Rule approach is reapplied, but with the second and third time intervals ($\Delta t_{n+1}, \Delta t_{n+2}$), respectively. Generally, the modified approach gives us the area under the curve for a single interval (Δa_m) using its and the following corresponding time intervals to generate the curve ($\Delta t_m, \Delta t_{m+1}$). This modified approach allows additional flexibility by making more individual $\Delta a/\Delta t$ sub-intervals available in evaluating linear regression values. Such evaluation permits the optimum limits of linear portions in the autocatalytic rate plot to be determined where a single coherent mechanistic kinetic step produces a kinetic rate constant (k). A software program

using a modification of the Simpson's Rule was written and developed to calculate α , Δa , a , and A values for the decomposed DNNC samples.

3. Results and Discussion

IDSC measurements taken with maximum instrument sensitivity at 142, 145, and 148 °C reveal that a very slow exothermic solid state DNNC thermochemical decomposition proceeds below its 155-156 °C melting point. Both the endothermic induction period time and exothermic decomposition rate constant data obtained from IDSC curves for DNNC and DNNC-d₆ show a positive kinetic deuterium isotope effect (KDIE). Comparative superimposed decomposition curves taken at 148 °C qualitatively illustrate this positive KDIE where the DNNC decomposition rate proceeds significantly more rapidly than for DNNC-d₆ (Fig. 3). KDIE details identify the rate-controlling step which is a mechanistic feature very important in regulating energetic compound behavior.[13,14]

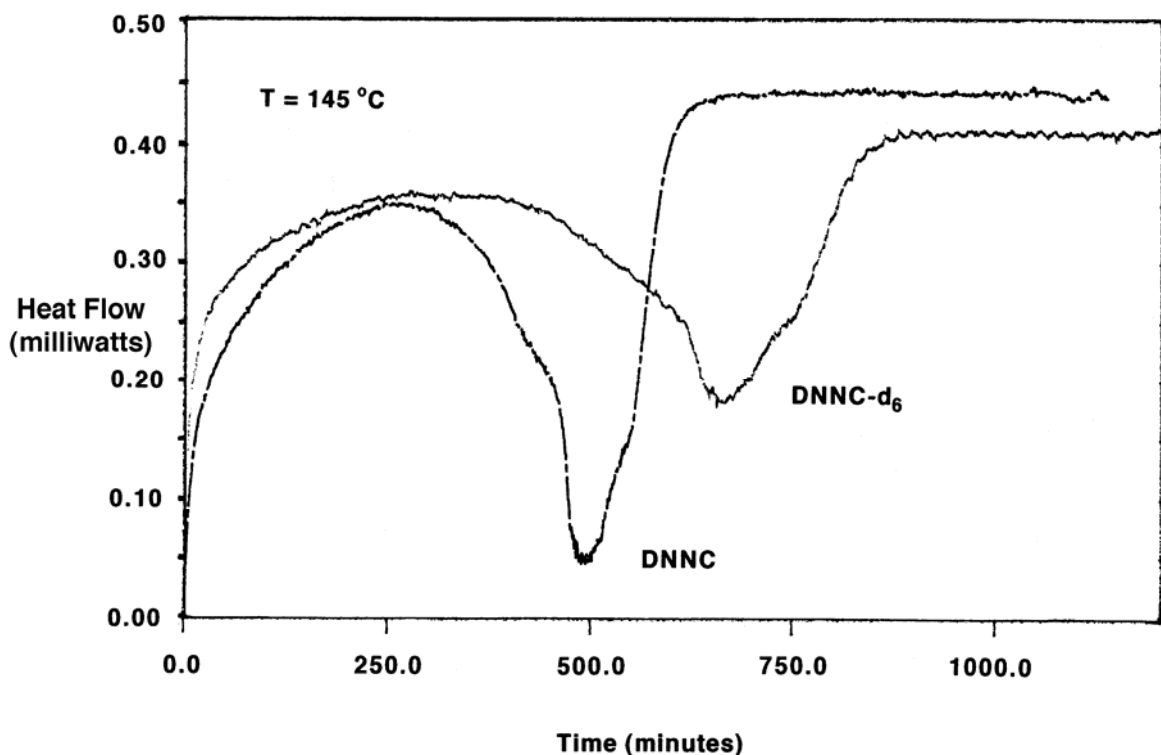


Fig. 3. Real-time IDSC decomposition curve comparison of DNNC and DNNC-d6 runs at 145 °C.

3.1 Physicochemical Characteristics

IDSC analyses of DNNC taken at 142, 145, and 148 °C revealed a lengthy three (184 min. at 148 °C) to nearly five hour (293 min. at 142 °C) endothermic induction period. This induction period was then followed by an exothermic thermochemical decomposition process (Fig. 4) whose autocatalytic rate plot displays three linear segments from which rate constant data could be obtained as illustrated later in Fig. 6. The time required for the solid state decomposition process differs markedly from the liquid state process. For example, liquid state DNNC decomposition at 176 °C is complete in about 42 minutes (0.7 hours)[9,12] while its entire solid state decomposition process at 145 °C requires nearly 14 hours or 20 times longer.

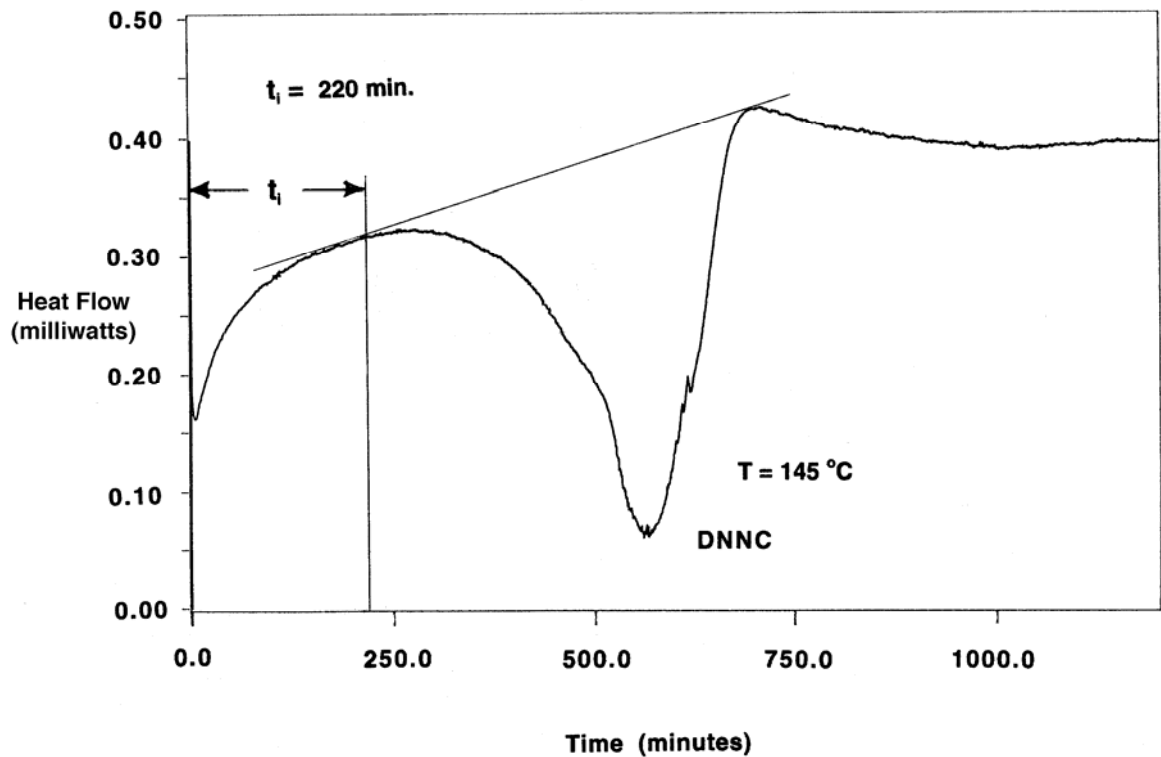


Fig. 4. Induction period (t_i) analysis for a DNNC run at 145 °C.

Although the thermochemical stability and explosive initiation sensitivity of DNNC more closely resembles that of TNT, the chemical reaction behavior of the solid state DNNC thermochemical decomposition process falls somewhere between its cyclic saturated RDX or HMX nitramine relatives and aromatic TNT.

Over the entire solid state decomposition process, both DNNC and DNNC- d_6 lose an average of 75 percent sample mass to gaseous product formation and evolution (Table 1). Student t statistical analyses of the data in Table 1 confirm that all weight loss values are the same number at a 99.5 confidence correlation. This average weight loss, obtained from 32 sample runs, shows approximately 25 percent of the original DNNC compound mass remains as condensed phase reaction product(s). In comparison, the HMX nitramine produces only

Table 1.

Solid State DNNC and DNNC-d₆ Thermochemical Decomposition Mass Losses

| Compound | Temperature (°C) | Mass Loss (%) | Standard Deviation |
|---------------------|------------------|-------------------------|--------------------|
| DNNC | 148 | 78.5 | ± 5.1 |
| DNNC-d ₆ | 148 | 74.7 | ± 1.8 |
| DNNC | 145 | 75.5 | ± 3.3 |
| DNNC-d ₆ | 145 | 71.7 | ± 1.4 |
| DNNC | 142 | 75.2 | ± 1.5 |
| DNNC-d ₆ | 142 | <u>72.9</u> | ± 1.3 |
| | | Ave. Mass Loss = 74.8 % | |

gaseous decomposition products leaving no significant condensed phase material after complete decomposition,[17] while TNT mainly produces condensed phase decomposition products.[18, 28-30]

The presence of condensed decomposition products should instill some caution when evaluating KDIE values and assigning the homolytic bond rupture that controls the rate at which a thermochemical decomposition process proceeds. Condensed phase product formation introduces mechanistic consequences which potentially dilute or reduce a true primary KDIE value below its accepted 1.35 experimental minimum. This situation incorrectly can suggest a false secondary KDIE value in the 1.01 to 1.34 range.[13,18]

3.1 Kinetic and Mechanistic Characteristics

3.1.1 Endothermic Induction Period Curve Portion (A)

The endothermic induction period (t_i) seen in Fig. 4 can be evaluated for a kinetic deuterium isotope effect (KDIE) using a ratio of the DNNC-d₆ and DNNC induction times, t_{id}/t_{ih} . This was first demonstrated with the liquid TNT thermochemical decomposition process.[18].

Assuming a short temperature equilibration time during the induction period of the solid state DNNC sample, and that other non-kinetic crystal lattice or physicochemical factors are not present that might dilute or mask a true primary KDIE value, the t_{id}/t_{ih} induction period ratio reveals a KDIE equal to 1.21 (Table 2). Because assignment of the induction period termination point for each decomposition curve often is no more accurate than ± 10 minutes, the standard deviations at 148 and 145 °C can be treated as statistically significant.

Presupposing that a small concentration of catalytic species forms from DNNC, which then

Table 2.

KDIE Data for Induction Period (t_i) Portion of the Thermochemical Decomposition Process

| Compound | Temp. (°C) | t_i (min.) | Std. Dev. | KDIE (t_d/t_h) |
|---------------------|------------|--------------|-----------|---------------------|
| DNNC-d ₆ | 148 | 210 | ± 8 | ----- |
| DNNC | 148 | 184 | ± 18 | 1.14 |
| DNNC-d ₆ | 145 | 316 | ± 31 | ----- |
| DNNC | 145 | 251 | ± 19 | 1.26 |
| DNNC-d ₆ | 142 | 365 | ± 75 | ----- |
| DNNC | 142 | 293 | ± 67 | <u>1.23</u> |
| | | | | Overall KDIE = 1.21 |

initiates the autocatalytic exothermic solid state decomposition process, this secondary KDIE value would suggest the rate-controlling step occurs either by pendant N-NO₂, pendant C-NO₂, or more likely, ring C-N homolytic bond cleavage. Previous studies with the related RDX nitramine and larger HMX nitramine have addressed both possible N-NO₂ and ring C-N bond cleavage occurring during the decomposition process, but not as the rate-controlling step.[25-27,31-38] The one exception was a rate-controlling homolytic ring C-N bond rupture detected during the decay portion of the solid HMX decomposition process once the HMX entered into a liquid phase.[17]

Previously, a primary KDIE of 1.66 was found in the induction period for the liquid state TNT decomposition, and further HPLC investigation revealed a small concentration of catalytic species formed by a rate-controlling step involving pendant methyl group C-H bond rupture from the TNT itself. This rate-controlling homolytic C-H bond rupture required an activation energy equal to 194.6 kJ/mole. Upon reaching a threshold concentration, the catalytic species initiated the TNT exothermic decomposition.[18] Because the endothermic DNNC induction period transitions into an autocatalytic exothermic decomposition, induction period formation of a catalytic species from DNNC also could be possible.

Plotting $\ln t_i$ versus $1/T$ affords a 128.1 kJ/mole activation energy for the DNNC endothermic induction period with a 0.990 linear regression data correlation (Fig. 5). Interestingly, this solid state DNNC induction period activation energy is significantly lower than the analogous induction period activation energies found during the neat thermochemical decomposition process with liquid state DNNC (185.0 kJ/mole) [12] and liquid state TNT,

(194.6 kJ/mole)[18], where in both cases, homolytic C-H bond rupture was the rate-controlling step.

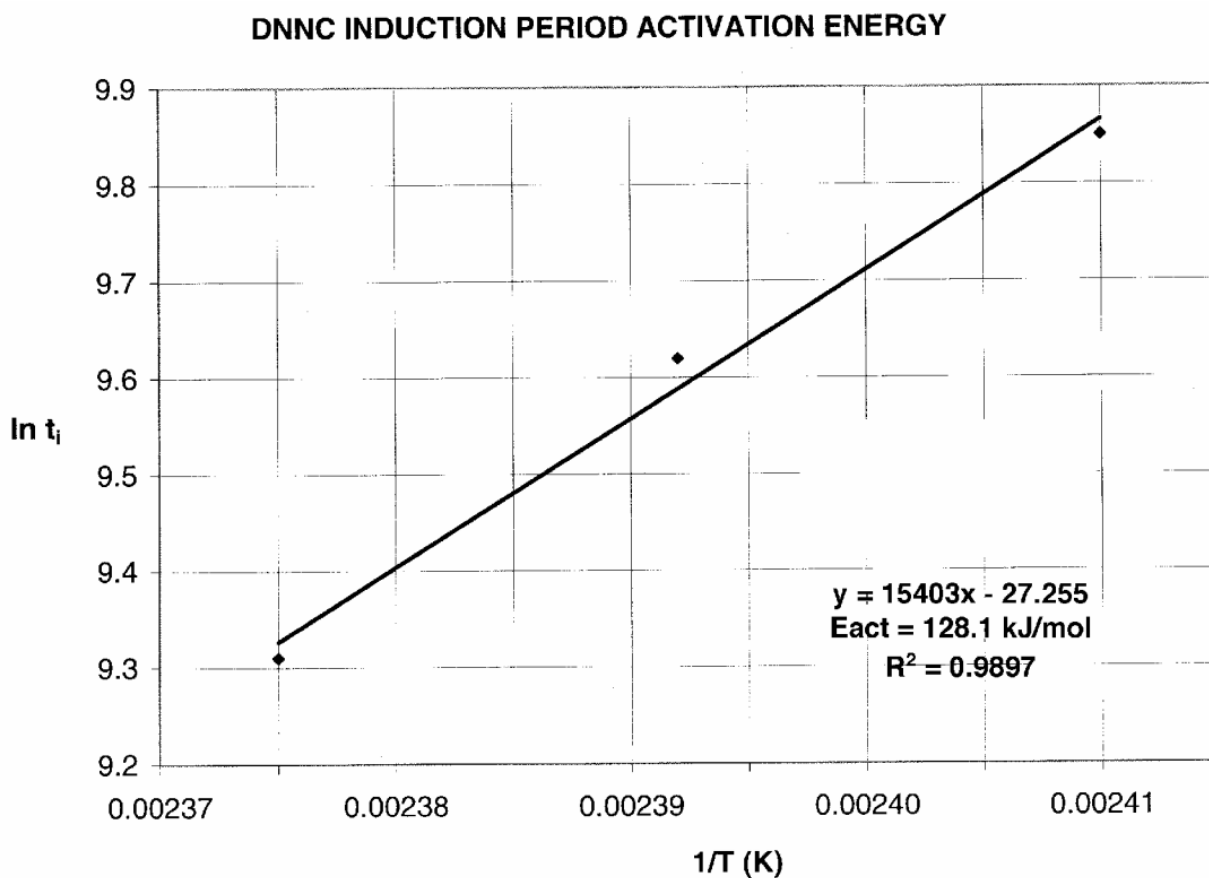


Fig. 5. Energy of activation for induction period of DNNC decomposition curve from 142 to 148 °C.

3.1.2 Exothermic Early Acceleratory Curve Portion

Following the endothermic induction period, a DNNC exothermic decomposition is initiated that follows an autocatalytic rate behavior. The autocatalytic rate plot reveals three linear segments for the DNNC and DNNC-d₆ at 145 and 148 °C (Fig. 6). These linear segments occur in the early acceleratory portion (A), the later acceleratory portion near the

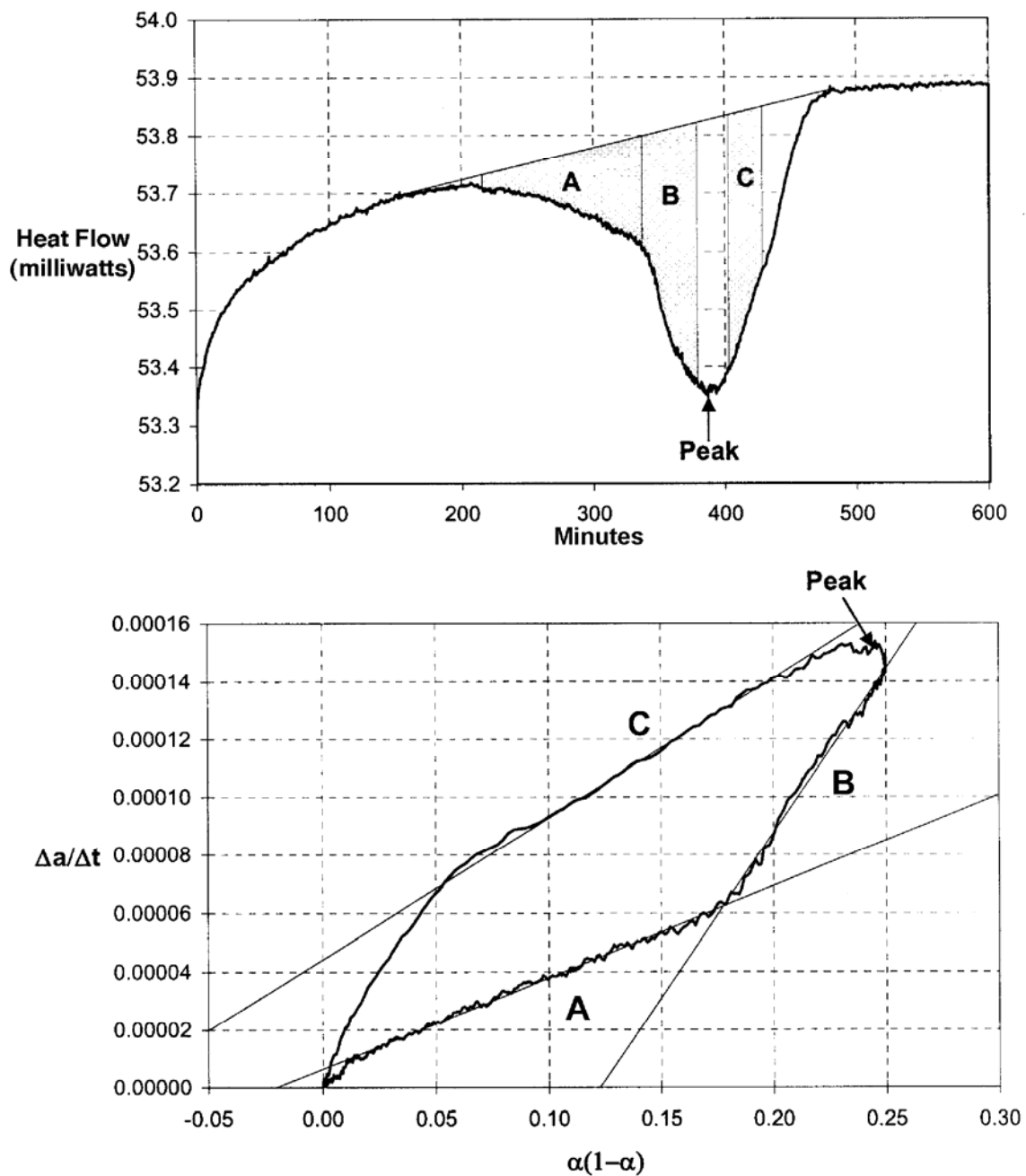


Fig. 6. Comparison of DNNC IDSC decomposition curve (top) obtained at 148 °C and corresponding autocatalytic rate plot (bottom).

maximum heat release peak (B), and in the decay portion (C) of the decomposition curve.

The slope of these three linear portions can provide rate constant (k) data where an

exothermic coherent, steady-state process occurs from one predominating reaction pathway.[17] At the lowest 142 °C temperature, only the early acceleratory (A) and decay portions (C) of the exothermic decomposition curve show linearity. Linearity in the later acceleratory portion (B) disappears and may not be kinetically driven. Combining these two or three linear segment percentages for each curve, the total percent that the thermogram curves follow autocatalytic rate kinetics, within the 142 to 148 °C temperature spread, is quite high ranging from 62 to 66 percent for DNNC and 64 to 76 percent for DNNC-d₆.

The extended 10 to 14 hour duration, covered by the solid state DNNC decomposition process, coupled with limited number of data points the IDSC instrument can store, suggested that more accurate partial $\Delta a/\Delta t$ curve area measurements, than previously used, might be necessary. A more rigorous increment-based autocatalytic rate plot program, described in the Experimental section, was developed to obtain the reaction rate constants, and derived KDIE values presented in this article.

Several IDSC runs were evaluated using a formerly reported height-based approximation to obtain the $\Delta a/\Delta t$ values comprising the autocatalytic rate plot.[16] Although an approximation, the height-based autocatalytic rate constant values are surprisingly similar to those obtained using the newer increment-based autocatalytic rate program used in this investigation (Table 3) and suggest this approximation is quite reasonable.

Table 3.

Height-Based vs. Increment-Based DNNC Autocatalytic Plot Rate Constants^(a) at 148 °C

| Method | Early Acceleration (A) | Later Acceleration (B) | Decay Phase (C) |
|-----------------|------------------------|------------------------|-----------------|
| Height-Based | 3.25 ± 0.23 | 9.06 ± 1.71 | 4.49 ± 0.45 |
| Increment-Based | 3.28 ± 0.25 | 8.94 ± 1.73 | 4.58 ± 0.48 |

^a Rate constant values x 10⁻⁴ sec⁻¹.

± Data variations represent one standard deviation.

Table 4 illustrates the more rigorous increment-based autocatalytic rate constant values obtained at 142, 145, and 148 °C during the early exothermic acceleratory portion (A) of the DNNC and DNNC-d₆ decomposition processes. Particularly noteworthy are the exceptionally high linear regression correlation values for the autocatalytic rate plots.

The early exothermic acceleratory portion (A) provides an average KDIE value equal to 1.47 over the 142 to 148 °C temperature range and strongly suggests a primary KDIE is present. This 1.47 value comes from linear fits to the autocatalytic rate plot that afford very impressive 0.998 (DNNC) and 0.994 (DNNC-d₆) least squares fitted correlation factors (R²). This primary 1.47 KDIE value for (A) suggests that homolytic C-H bond rupture, in one type or both types of chemically non-equivalent DNNC methylene groups, constitutes the rate-controlling step. The 1.47 value comfortably exceeds the theoretical high temperature lower limit of 1.41 and the experimentally accepted 1.35 lower limit for a primary KDIE. [13,17-19] Assignment of a primary KDIE further is supported by a mathematically normalized KDIE value of 2.52 at standard 298 K (25 °C) temperature calculated from the experimental 1.47

KDIE value using an average decomposition temperature of 145 °C.[39] At 25 °C, a 2.5 value constitutes the accepted minimum threshold for a primary KDIE.[40] This linear early

Table 4.

Kinetic Data for Early Acceleratory Portion (A) of the Thermochemical Decomposition Process

| Compound | Temp. (°C) | $k \times 10^{-4} \text{ (s}^{-1}\text{)}$ | Std. Dev. $\times 10^{-4}$ | KDIE | R^2 |
|---------------------|------------|--|----------------------------|---------------------|-------|
| DNNC | 148 | 3.38 | ± 0.24 | ----- | 0.998 |
| DNNC-d ₆ | 148 | 2.51 | ± 0.16 | 1.35 | 0.994 |
| DNNC | 145 | 3.13 | ± 0.36 | ----- | 0.997 |
| DNNC-d ₆ | 145 | 2.02 | ± 0.14 | 1.55 | 0.995 |
| DNNC | 142 | 2.36 | ± 0.10 | ----- | 0.998 |
| DNNC-d ₆ | 142 | 1.56 | ± 0.26 | <u>1.51</u> | 0.995 |
| | | | | Overall KDIE = 1.47 | |

R^2 = Linear correlation fit to early acceleratory portion of the autocatalytic rate plot.

acceleratory portion (A) for DNNC constitutes 16 to 18 percent of the total decomposition curve at 148 and 145 °C respectively, but noticeably increases to 38% at 142 °C (Table 5).

The DNNC-d₆ energy of activation was determined for this exothermic early acceleratory portion (A) of the decomposition process. By plotting its respective rate constant logarithm against each corresponding reciprocal temperature (Fig. 7), a 115.2 kJ/mole activation energy for DNNC-d₆ was obtained with an exceptional 0.998 linear regression correlation (R^2). If the rate-controlling methylene C-H bond rupture occurs during the activation step, a lower energy of activation for unlabeled DNNC should result. Because the ground state zero

vibrational energy difference between the C-H and the stronger C-D bond is 9.6 kJ/mole (2.3 kcal/mole), the DNNC activation energy then would be expected to be 9.6 kJ/mole less than DNNC-d₆ or

Table 5.

Percent of IDSC Decomposition Curve covered by the Linear Early Acceleratory Portion (A)

| Compound | Temperature (°C) | % Decomposition | Std. Deviation | R ² |
|---------------------|------------------|-----------------|----------------|----------------|
| DNNC | 148 | 16.7 | ± 7.9 | 0.998 |
| DNNC-d ₆ | 148 | 16.2 | ± 5.6 | 0.994 |
| DNNC | 145 | 18.2 | ± 6.3 | 0.997 |
| DNNC-d ₆ | 145 | 26.9 | ± 5.1 | 0.995 |
| DNNC | 142 | 37.6 | ± 3.1 | 0.998 |
| DNNC-d ₆ | 142 | 39.5 | ± 4.9 | 0.994 |

R² = Linear correlation fit to early acceleratory portion of the autocatalytic rate plot.

around 105.6 kJ/mole. An analogous energy of activation plot of Fig. 6 for DNNC gave an activation energy equal to 87.1 kJ/mole, but with only a lower 0.904 linear regression correlation. Considering this much lower linear regression correlation, the DNNC 105.6 kJ/mole energy of activation data appears to be more reasonable and reliable. This 105.6 kJ/mol activation energy is about 22 kJ/mole lower than the 128.1 kJ/mole activation energy for the DNNC induction period. This point further supports the possibility that a small threshold concentration of catalytic species forms from DNNC during the endothermic induction period to lower the decomposition activation energy and initiate the exothermic

acceleratory decomposition. If this is so, the catalytic species forms by a different rate-limiting step than the C-H bond rupture that controls the energy release rate during the entire exothermic decomposition process. With its higher endothermic induction period activation

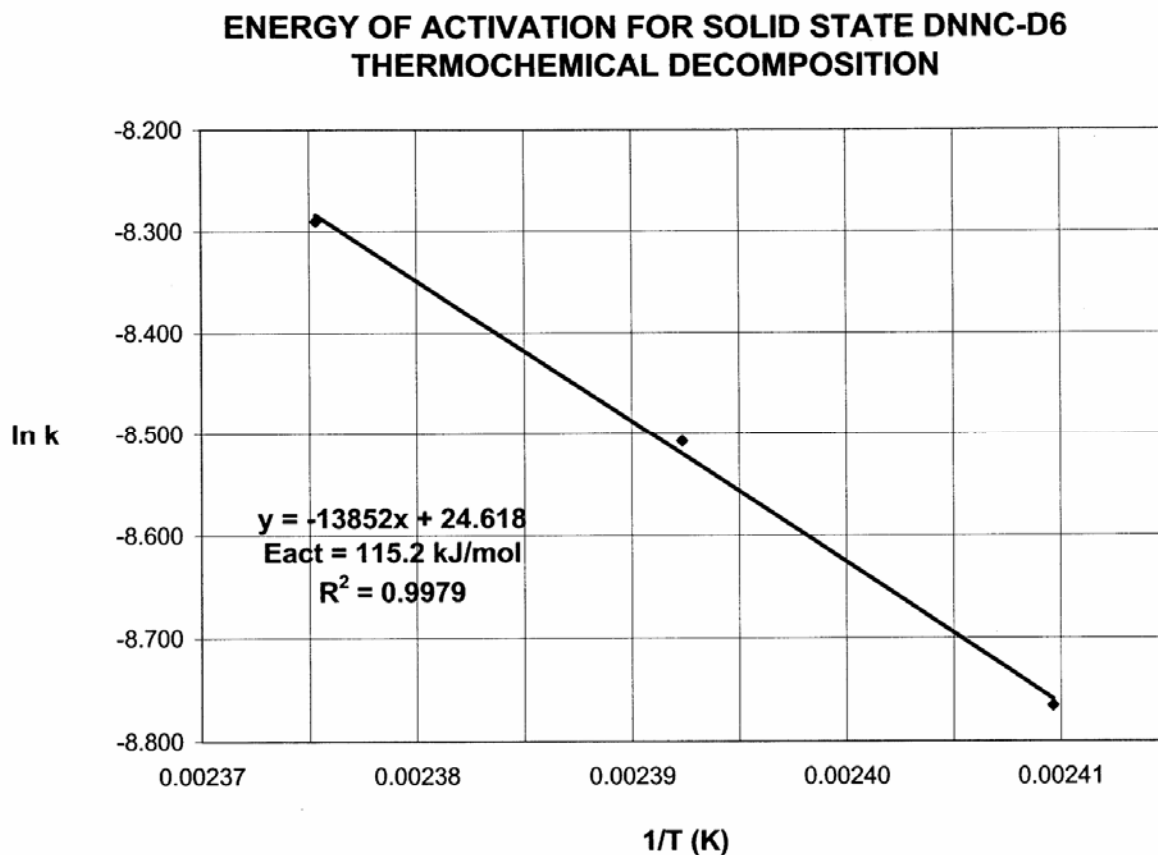


Fig. 7. Energy of activation for early exothermic acceleratory portion [A] of DNNC-d₆ decomposition curve from 142 to 148 °C.

energy, and a lower energy of activation for the exothermic early acceleratory decomposition, DNNC mirrors the same activation energy pattern as TNT where a small amount of TNT converts to a catalytic species that initiates its exothermic decomposition process. Coupled with the autocatalytic nature of the DNNC decomposition process, this same energy of activation pattern further supports the possibility of catalytic species formation during the DNNC induction period.

3.1.2 Exothermic Later Acceleratory Curve Portion (B)

The latter acceleratory portion (B) for the solid-state DNNC and DNNC-d₆ decomposition process (Figure 6) appears to give an average primary KDIE value of 1.64 at 148 °C and 145 °C. The linear segment of the autocatalytic rate plot covers 22 to 26 percent of the total decomposition curve at the 148 °C, decreases to 10 to 14 percent at 145 °C, and disappears at 142 °C. This linear segment also reveals a very unusual characteristic indicating the decomposition process at this point is influenced by some factor other than normal kinetics behavior (Table 6). The “apparent” rate constant, obtained at 148 °C and 145 °C, increases at the lower temperature with both DNNC and DNNC-d₆. We have no current explanation for this very unusual result, and dismiss this data as being generated by pure kinetic behavior.

Table 6.

Kinetic Data for Later Acceleratory Portion (B) of the Thermochemical Decomposition Process

| Compound | Temp. (°C) | k x 10 ⁻⁴ (s ⁻¹) | Std. Dev. x 10 ⁻⁴ | KDIE | R ² |
|---------------------|------------|---|------------------------------|---------------------|----------------|
| DNNC | 148 | 8.70 | ± 0.36 | ----- | 0.997 |
| DNNC-d ₆ | 148 | 5.45 | ± 0.95 | 1.60 | 0.997 |
| DNNC | 145 | 14.74 | ± 0.47 | ----- | 0.994 |
| DNNC-d ₆ | 145 | 8.74 | ± 0.34 | <u>1.69</u> | 0.984 |
| | | | | Overall KDIE = 1.64 | |

R² = Linear correlation fit to early acceleratory portion of the autocatalytic rate plot.

3.1.3 Exothermic Decay Curve Portion

The decay portion (C) of the DNNC thermochemical decomposition provides a k_h/k_d KDIE rate constant ratio equal to 1.27 (Table 7). This linear segment of the autocatalytic rate plot covers 22 to 34 percent of the total decomposition curve for DNNC and a similar 26 to 34 percent for DNNC- d_6 . By magnitude alone, the 1.27 value could suggest a secondary KDIE since it falls within a 1.01 to 1.34 experimental range and would be a change in the rate-controlling mechanistic step from the homolytic C-H bond cleavage observed in the early acceleratory portion (A). This is the case for the HMX nitramine, where the rate-controlling C-H bond rupture defines the rate-controlling solid state decomposition, but then transitions to a rate-controlling ring C-N bond cleavage in its liquefied state.[17] Unlike DNNC, however, HMX essentially leaves no condensed phase byproduct(s) when its decomposition process

Table 7.

Kinetic Data of the Decay Portion (C) of the Thermochemical Decomposition Process

| Compound | Temp. (°C) | $k \times 10^{-4} (s^{-1})$ | Std. Dev. $\times 10^{-4}$ | KDIE | R^2 |
|-------------|------------|-----------------------------|----------------------------|---------------------|-------|
| DNNC | 148 | 4.36 | ± 0.52 | ----- | 0.996 |
| DNNC- d_6 | 148 | 3.52 | ± 0.65 | 1.24 | 0.992 |
| DNNC | 145 | 3.13 | ± 0.32 | ----- | 0.988 |
| DNNC- d_6 | 145 | 2.78 | ± 0.78 | 1.13 | 0.973 |
| DNNC | 142 | 2.19 | ± 0.46 | ----- | 0.976 |
| DNNC- d_6 | 142 | 1.53 | ± 0.36 | <u>1.43</u> | 0.970 |
| | | | | Overall KDIE = 1.27 | |

R^2 = Linear correlation fit to early acceleratory portion of the autocatalytic rate plot.

is complete. The presence of 25 percent condensed phase DNNC decomposition product

residue, after completion of the exothermic decomposition process, introduces the possibility

that a primary KDIE value for decay portion (C) is being reduced or diluted to the magnitude associated with a secondary KDIE. Reactions that form these condensed phase products by a rate-controlling step not involving C-H bond rupture can account for this behavior. Such a dilution of a primary KDIE value has been documented in the decay portion of both the liquid state TNT[13,18] and solid state TATB[3,13,24] decomposition processes. Secondly, even if the DNNC samples transitioned into the liquid state during this decay portion, KDIE thermochemical decomposition studies conducted on liquid DNNC and DNNC-d₆ show no evidence of a secondary KDIE.[12,41] This further suggests the 1.27 KDIE value for the DNNC decay portion (C) of the IDSC thermogram, likely is a diluted primary KDIE value. If so, once initiated, homolytic C-H bond rupture constitutes the rate-controlling throughout the entire exothermic DNNC decomposition process.

3.2 Mechanistic Summary

The possible endothermic induction period formation of a catalytic species from DNNC itself, theoretically could result from either a pendant N-NO₂, pendant C-NO₂, but most likely a ring C-N rate-controlling bond rupture suggested by the secondary 1.21 KDIE value. A plethora of past cyclic nitramine decomposition data show that pendant N-NO₂ homolysis, the weakest bond in the nitramine molecule, initiates the decomposition process, followed by a C-N bond rupture which could be rate-controlling. A former DNNC study suggests that either pendant C-NO₂, or possibly N-NO₂ bond rupture (the DNNC molecule's two weakest bonds) is the first step that determines the decomposition reaction pathway which subsequently involves a ring C-N bond cleavage step.[4] Once formed in a threshold concentration, a possible catalytic species then could initiate the solid state DNNC exothermic thermochemical decomposition where the rate controlling step transitions from a

possible C-N ring bond rupture to C-H bond rupture. The 1.47 primary KDIE value for the early exothermic acceleratory portion (A) reveals this rate-controlling C-H bond rupture transition which appears to regulate the rest of the exothermic decomposition process.

Past mechanistic IDSC-based KDIE thermochemical decomposition studies of liquid state TNT,[18] solid state TATB,[3] solid state HMX,[15] and liquid state RDX[19] clearly reinforce the mechanistic importance that the early portion of the thermochemical decomposition curve contributes to the overall decomposition process. KDIE values obtained from a thermogram curve, either during an induction period or during the early acceleratory phase, reveal the key mechanistic rate-controlling step that determines the overall decomposition rate. These regions of the IDSC thermogram curve, corresponding to the early portions of the thermochemical decomposition process, are least affected by additional complicating mechanistic factors.

The results of this study support a previous neat DNNC thermochemical decomposition investigation where plausible mechanistic proposals were discussed. The mechanistic proposals were based upon gaseous products generated under bimolecular decomposition conditions representative of a burning surface.[4] Proposed from this gaseous product study was a three-stage process involving three possible and competing DNNC mechanistic decomposition pathways. While many plausible secondary decomposition reactions could occur either from an initial C-NO₂ (5-position) or N-NO₂ (1- and 3-positions) homolytic bond rupture, predominant initiation via C-NO₂ homolysis was selected for mechanistic discussion purposes.[4] An endothermic first stage suggests that NO₂ radical formation, from C-NO₂ homolysis, could be followed by two different subsequent reaction pathways where each contains a homolytic ring C-N bond rupture. The appearance of a secondary KDIE, during

the endothermic induction period in our IDSC study of the solid state DNNC decomposition process, is consistent with either of these previously suggested pathways and shows homolytic C-N bond rupture could be the rate-controlling step during this early first stage.

Next in the previous DNNC decomposition study, an exothermic second stage is described which causes a sharp increase in NO and NO₂ gaseous products. This behavior is consistent with the primary KDIE we observed during the early exothermic acceleratory portion (A) of the IDSC thermogram where C-H bond homolysis, possibly at the 2- or 4-position, becomes the predominating rate-controlling step. Following an initial C-NO₂ or N-NO₂ bond homolysis to produce the NO₂ radical, subsequent NO₂ radical abstraction of a methylene hydrogen atom from the remaining cyclic DNNC ring structure would form HONO,[17] an unstable molecule where two moles decompose into one mole of NO, NO₂, and H₂O gaseous products. A subsequent C-N ring opening, adjacent to the lower energy allylic ring nitrogen at the 1- or 3-position in the cyclic DNNC fragment, is consistent with a third reaction pathway suggested.[4]

Rate-controlling C-H homolysis, occurring late in the decay portion (C) of our decomposition process, also is consistent with the previously discussed third stage where a small amount of HONO was found.[4] Bimolecular recombination reactions would produce the observed condensed phase residue[4] found in the IDSC pans once the solid state thermochemical decomposition process is complete (Table 1). The late third stage appearance of HONO, and nonvolatile condensed phase residue formation by other reactions, possibly not involving a C-H rate-controlling bond rupture, further suggests the 1.27 KDIE value seen in the late decay portion (C) of the IDSC thermogram was a masked or diluted primary KDIE value.

As previously noted, initial N-NO₂ homolysis cannot be ruled out.[4] An NO₂ radical formation from N-NO₂ homolysis, a subsequent rate-controlling hydrogen atom abstraction from the methylene at the 2-position (eg. C-H bond rupture) to form unstable HONO, followed by a subsequent ring opening, like that proposed for HMX,[17] also could explain the second and third stage[4] gaseous products previously reported.[4] Additionally, this alternative pathway would be consistent with the primary KDIE found in this study during the exothermic acceleratory portion of the decomposition process.

4. Conclusions

The early portion the DNNC/DNNC-d₆ thermochemical decomposition process clearly exerts a major role in determining the specific chemical bond rupture that controls the energy release rate of the decomposition process. This point is reflected in previously-reported mechanistic KDIE-based IDSC thermochemical decomposition investigations with liquid state TNT/TNT- α -d₃, solid state TATB/TATB-d₆, solid state HMX/HMX-d₈, and liquid state RDX/RDX-d₆.

Within the temperature range investigated, a secondary 1.21 KDIE value for the initial endothermic induction period in DNNC thermochemical decomposition behavior likely indicates a rate-controlling ring C-N bond cleavage could be forming a catalytic species, which upon reaching a small threshold concentration, initiates its subsequent autocatalytic exothermic energy release rate behavior. A lower 105.6 kJ/mol activation energy for the subsequent autocatalytic exothermic decomposition, following a higher induction period 128.1 kJ/mol activation energy, further supports endothermic induction period formation of a catalytic species from DNNC itself. This same mechanistic behavior previously was reported

for the liquid TNT decomposition process which followed the same energy of activation pattern. The endothermic induction period results are consistent with a previously suggested mechanistic pathway for the first stage DNNC decomposition process found in a representative burning surface.

Upon initiating the exothermic thermochemical decomposition process, the early acceleratory portion (A) of the DNNC decomposition curve shows a 1.47 KDIE value suggesting that the rate-controlling step transitions to a C-H bond rupture at one or both types of chemically non-equivalent ring methylene groups in DNNC molecule. This rate-controlling C-H bond homolysis likely predominates throughout the remaining exothermic decomposition process. Again, this result supports previously proposed mechanistic pathways for an exothermic second and third stage DNNC surface decomposition process that simulates surface combustion conditions. The DNNC 105.6 kJ/mol activation energy in the early exothermic acceleratory portion (A) for decomposition process can be obtained from a measured 115.2 kJ/mol DNNC-d₆ activation energy.

Acknowledgments

Dedicated to the memory of Raymond N. Rogers (Los Alamos National Laboratory), a pioneer in isothermal DSC kinetic analysis, an outstanding scientist, a research mentor, collaborator, and true friend (dec. Mar 8, 2005)-SAS.

The authors gratefully thank the following individuals: Dr. Kenneth A. Martin, Dr. Victor L. Heasley, and Dr. Dale F. Shellhamer, Department of Chemistry, Pt. Loma Nazarene University, San Diego, CA, for helpful scientific discussions, key software support, and on-

site computer assistance in the preparation of this manuscript. Mr. Dean Richards, AF Research Laboratory (AFRL), Edwards AFB, CA, provided critical computer graphics support. Dr. Jerry Boatz (AFRL) and Dr. Karl O. Christe (AFRL) contributed pertinent technical comments and discussion during manuscript preparation. Dr. John Belletire and Dr. Jeff Mills provided critical review of the written manuscript. The Air Force Office of Scientific Research (AFOSR) is gratefully acknowledged for funding this research study.

5. References

- [1] (a) Present address: Donald Bren School of Information and Computer Sciences, University of California, Irvine, Irvine, CA 92697 (USA).
(b) Experimental IDSC thermochemical decomposition investigations were conducted at The F. J. Seiler Research Laboratory, USAF Academy, CO (USA) prior to its Sep 30, 1995 decommissioning.
(c) Adjunct Professor, Pt. Loma Nazarene University, San Diego, CA, Aug 1997 to Aug 2003.
- [2] A. K. Galwey, M. E. Brown, *Thermal Decomposition of Ionic Solids*, Elsevier, Amsterdam, , 1999, Chap. 1, pp. 1-2.
- [3] R. N. Rogers, J. L. Janney, M. H. Ebinger, *Thermochim. Acta*, 59 (1982) 287-298.
- [4] T. B. Brill, D. G. Patil, J. Duterque, G. Lengelle, *Combust. Flame*, 95 (1993) 183-190.
- [5] S. A. Shackelford, B. B. Goshgarian, R. D. Chapman, R. E. Askins, D. A. Flanigan, R. N. Rogers, *Propellants, Explos. Pyrotech.*, 14 (1989) 93-102.
- [6] D. L. Levins, C. D. Bedford, and C. L. Coon, U.S. Patent 4,346,222 (1982) SRI International, USA.
- [7] D. A. Cichra and H. G. Adolph, *J. Org. Chem.*, 47 (1982) 2472-2476.
- [8] J. Boileau, M. Piteau, and G. Jacob, *Propellants, Explos. Pyrotech.*, 15 (1990) 38. The subject DNNC compound also has appeared in the literature under the acronym of TNDA.
- [9] S. A. Shackelford and J. F. Goldman, *Propellants, Explos., Pyrotech.*, 20 (1995) 1-4, and references cited therein.
- [10] J. Wang, K. R. Brower, D. L. Naud, *J. Org. Chem.*, 62 (1997) 9055-9060.

- [11] B. D. Roos, T. B. Brill, *Propellants, Explos., Pyrotech.*, 28 (2003) 65-71.
- [12] S. A. Shackelford, J. F. Goldman, J. A. Menapace, S. A. Hendrickson, 35th Int. Ann. Conf. of ICT, Karlsruhe, Germany, June 29-July 2, 2004.
- [13] S. A. Shackelford, in *Chemistry and Physics of Energetic Materials*, ed. S. N. Bulusu, NATO ASI Series, Series C, Vol 309, Kluwer Academic Press, Dordrecht, NL, 1990, Chap. 18, pp.413-432 & Chap.19, pp. 433-456
- [14] S. A. Shackelford, *J. de Physique IV*, Colloque C4, suppl. to *J. de Physique III*, 5 (1995) 485-499.
- [15] S. A. Shackelford, *J. Labeled Comps. and Radiopharm.*, XXIX (1991) 1197-1206.
- [16] R. N. Rogers, RCEM Rpt. A-04-87, Research Center for Energetic Materials, New Mexico Tech., Socorro, NM, USA 87081, Nov. 4, 1987, pp. 15-65,.
- [17] S. A. Shackelford, M. B. Coolidge, B. B. Goshgarian, B. A. Loving, R. N. Rogers, J. L. Janney, M. H. Ebinger, *J. Phys. Chem.*, 89 (1985) 3118-3126.
- [18] S. A. Shackelford, J. W. Beckmann, J. S. Wilkes, *J. Org. Chem.*, 42 (1977) 4201- 4206.
- [19] S. L. Rodgers, M. B. Coolidge, W. J. Lauderdale, S. A. Shackelford, *Thermochim. Acta*, 177 (1991) 151-168.
- [20] S. N. Bulusu, D. J. Weinstein, J. R. Autera, R. W. Velicky, *J. Phys. Chem.* , 90 (1986) 4121-4126.
- [21] S. A. Shackelford, S. L. Rodgers, R. E. Askins, *Propellants, Explos. Pyrotech.* , 16 (1991) 279-286.
- [22] S. N. Bulusu, J. R. Autera, *J. Energetic Matls.*, 1 (1983) 133-140.
- [23] J. Sharma, W. L. Garrett, F. J. Owens, V. L. Vogel, *J. Phys. Chem.*, 86 (1982) 1657-1661.
- [24] J. Sharma, J. C. Hoffsommer, D. J. Glover, C. S. Coffey, F. Santiago, A. Stolovy, S. Yasuda, in *Shock Waves in Condensed Matter*, eds. J. R. Asay, R. A. Graham , G. K. Straub, Elsevier, 1984, pp. 543-546.
- [25] J. Sharma, J. C. Hoffsommer, D. J. Glover, C. S. Coffey, J. W. Forbes, T. P. Liddiard, W. L. Elban, F. Santiago, 8th Intl. Symp. on Detonation, Albuquerque, NM, July 15-19, 1985.

- [26] J. Sharma, J. W. Forbes C. S. Coffey, T. P. Liddiard, *J. Phys. Chem.*, 91 (1987) 5139-5144.
- [27] J. Sharma, J. W. Forbes, C. S. Coffey, T. P. Liddiard, in *Shock Waves in Condensed Matter*, eds. S. C. Schmidt, N. C. Holmes, Elsevier, 1988, pp. 565-568.
- [28] L. A. Wiseman, Bristol Research Ret. No. 51, A. C. 2670, Ministry of Supply, Great Britain, 1942.
- [29] R. N. Rogers, *Anal. Chem.*, 39 (1967) 730-733.
- [30] J. C. Dacons, H. G. Adolph, M. J. Kamlet, *J. Phys. Chem.*, 74 (1970) 3035-3040.
- [31] J. D. Cosgrove, A. J. Owen, *Comb. Flame*, 22 (1974) 19-22.
- [32] M. A. Schroeder, in *Proceed. 16th JANNAF Combustion Meeting*, Monterey, CA, CPIA, The Johns Hopkins Univ., Laurel, MD, CPIA Publ. No. 308, 1979, Vol. II, pp. 17-34;
- [33] M. D. Pace, A. D. Britt, W. B. Moniz, *J. Energetic Matls.*, 1 (1983) 141-175.
- [34] R. A. Fifer, in *Fundamentals of Solid Propellant Combustion*, eds. K. K. Kuo, M. Summerfield, *Progress in Astronautics and Aeronautics*, 1984, Vol 90, AIAA, Inc., pp. 178-237.
- [35] R. Shaw, F. E. Walker, *J. Phys. Chem.*, 81 (1977) 2572-2576.
- [36] J. Kimura, N. Kubota, *Prop. Explos.*, 5 (1980) 1-8.
- [37] A. D. Britt, M. D. Pace, W. B. Monitz, *J. Energetic Matls.*, 1 (1983) 367-371.
- [38] Y. Shu, B. L. Korsounskii, G. M. Nazin, *Russ. Chem. Rev.*, 73 (2004) 293-307.
- [39] T. H. Lowery, K. S. Richardson, *Mechanism and Theory in Organic Chemistry*, Harper and Row, 2nd edn., New York, 1981, pp. 206-207.
- [40] G. W. Klump, *Reactivity in Organic Chemistry*, L. Birladeanu, (transl.), Wiley Interscience, New York, 1982, p. 262.
- [41] S. A. Shackelford, J. F. Goldman, 203rd Nat. Am. Chem. Soc. Mtg., San Francisco, CA (USA), April 5-10, 1992; and, S. A. Shackelford, J. F. Goldman, 22nd Int. Ann. Conf. of ICT, Karlsruhe, Germany, July 2-5, 1991.

